



Research Article

# Mesoporous Magnesium Oxide Adsorbent Prepared *via* Lime (*Citrus aurantifolia*) Peel Bio-templating for CO<sub>2</sub> Capture

A.H. Ruhaimi<sup>1</sup>, C.C. Teh<sup>1</sup>, Muhammad Arif A. Aziz<sup>1,2,\*</sup>

<sup>1</sup>School of Chemical and Energy Engineering, Faculty of Engineering, Universiti Teknologi Malaysia (UTM), 81310 UTM Johor Bahru, Johor, Malaysia.

<sup>2</sup>Centre of Hydrogen Energy, Institute of Future Energy, Universiti Teknologi Malaysia (UTM), 81310 UTM Johor Bahru, Johor, Malaysia.

Received: 2<sup>nd</sup> March 2021; Revised: 11<sup>th</sup> April 2021; Accepted: 12<sup>th</sup> April 2021  
Available online: 12<sup>nd</sup> April 2021; Published regularly: June 2021



## Abstract

The utilization of the lime (*Citrus aurantifolia*) peel as a template can improve the adsorbent's structural properties, which consequently affect its CO<sub>2</sub> uptake capacity. Herein, a mesoporous magnesium oxide (MgO-lime (*Citrus aurantifolia*) peel template (LPT)) adsorbent was synthesized using an LPT. MgO-LPT demonstrated improved structural properties and excellent CO<sub>2</sub> uptake capacity. Moreover, another MgO adsorbent was prepared via thermal decomposition (MgO-TD) for comparison. The prepared adsorbents were characterized by N<sub>2</sub> physisorption, Fourier transform infrared spectroscopy and thermogravimetric analysis. The CO<sub>2</sub> uptake of these adsorbents was under 100% CO<sub>2</sub> gas and ambient temperature and pressure conditions. MgO-LPT exhibited a higher Brunauer–Emmett–Teller surface area, Barrett–Joyner–Halenda pore volume, and pore diameter of 23 m<sup>2</sup>.g<sup>-1</sup>, 0.142 cm<sup>3</sup>.g<sup>-1</sup>, and 24.6 nm, respectively, than those of MgO-TD, which indicated the mesoporous structure of MgO-LPT. The CO<sub>2</sub> uptake capacity of MgO-LPT is 3.79 mmol CO<sub>2</sub>.g<sup>-1</sup>, which is 15 times that of MgO-TD. This study shows that the application of lime peel as a template for the synthesis of MgO adsorbents is a promising approach to achieve MgO adsorbents with enhanced surface area and thus increased CO<sub>2</sub> capture performance.

Copyright © 2021 by Authors, Published by BCREC Group. This is an open access article under the CC BY-SA License (<https://creativecommons.org/licenses/by-sa/4.0>).

**Keywords:** bio-templating; CO<sub>2</sub> capture; *Citrus aurantifolia*; lime peel template; magnesium oxide

**How to Cite:** A.H. Ruhaimi, C.C. Teh, M.A.A. Aziz (2021). Mesoporous Magnesium Oxide Adsorbent Prepared *via* Lime (*Citrus aurantifolia*) Peel Bio-templating for CO<sub>2</sub> Capture. *Bulletin of Chemical Reaction Engineering & Catalysis*, 16(2), 366-373 (doi:10.9767/bcrec.16.2.10505.366-373)

**Permalink/DOI:** <https://doi.org/10.9767/bcrec.16.2.10505.366-373>

## 1. Introduction

Conventional CO<sub>2</sub> separation methods (such as amine absorption) have several limitations, including high equipment corrosion rate, high regeneration cost, loss of solvent and low CO<sub>2</sub> loading capacity; thus, replacement of these methods with other CO<sub>2</sub> capture techniques

should be considered [1]. In this regard, one of the potential replacement methods is adsorption, which has been reported to possess promising advantages, for example, durability, easy regeneration, cost-effectiveness, and high adsorption capacity of the adsorbents [2,3]. Various adsorbents, such as zeolites, metal oxides, porous carbon, silica, metal-organic frameworks and covalent organic frameworks can be employed to achieve adsorption [4]. Each adsorbent possesses unique tuneable morphological and textural

\* Corresponding Author.  
Email: m.arif@utm.my (M.A.A. Aziz)

properties, which have been extensively studied to realize maximum CO<sub>2</sub> uptake capacity. Magnesium oxide (MgO) is a metal oxide adsorbent that has been widely investigated for achieving a high CO<sub>2</sub> uptake capacity due to its unique properties including appropriate surface basicity, a high theoretical uptake capacity of 24.8 mmol CO<sub>2</sub>.g<sup>-1</sup>, easy availability and non-toxicity [5,6]. However, the low surface area of common MgO results in a low CO<sub>2</sub> uptake capacity. Thus, numerous studies have been conducted to improve the surface area of MgO for realizing a high theoretical CO<sub>2</sub> uptake capacity.

Several fabrication approaches have been reported to improve the surface area of MgO, most of which involve the utilization of a surfactant as a porous generator. The most commonly used surfactant is cetyltrimethylammonium bromide [7,8]. Although various surfactants, such as sodium dodecyl sulfate, polyvinyl pyrrolidone, symmetric triblock copolymer (P123), and cetyltrimethylammonium chloride have been used to achieve high-surface-area adsorbents surfactant-utilizing methods are costly and complex [1,9]. Hence, the utilization of biomaterials as template sources for the fabrication of high-surface-area adsorbents can be a promising approach because biomaterials are abundantly available. Furthermore, biomaterial templating requires minimal reagents, thereby reducing the adsorbent preparation cost.

Many studies have reported the use of biomaterials, for instance, jute fibers, root hair, scallion root, and eggshell membranes [1] as templates to improve the physicochemical properties of metal oxide samples and consequently enhance the performances of these samples. For instances, Chen *et al.* has reported on the fabrication of the CuO via utilization plant root hair as a template [10]. Fabricated root hair-templated CuO has exhibited unique morphological features of the double hollow layer structure, which has resulted in the improvement of gas sensing performance. Moreover, Abarna *et al.* also reported on the utilization of plant-based material as a template which is jute fibre in the preparation of mesoporous ZnO [9]. It is found that jute fiber-templated ZnO has displayed an improvement of structural properties as compared to ZnO prepared without jute fiber. This enhanced ZnO's structural properties have contributed to the high ZnO photocatalytic efficiency. There are tremendous sources of bio-material that could be used as a template in synthesizing metal oxide adsorbent such as fruit peel waste. However, the use of

fruit peel waste, such as: citrus peel as a potential biomaterial template, has rarely been reported to date.

Various citrus species fruit peel can be used as templates. Each species may possess different morphological features. For example, although orange (*Citrus sinensis*) peel, citrus (*Citrus limetta*) peel, and lemon (*Citrus limon*) peel exhibit the same rough surface morphological features with numerous porous structures but their pore sizes are different. Another unique morphological feature of orange peel is that some fibrous structures are spread throughout its surface [11]. Moreover, citrus peel possesses several surface functional groups, including carboxyl, alcohol, aldehyde, ketone, alkene, amide, ester, and ether groups [11]. Thus, utilization of citrus fruit peel with interesting morphological characteristic as a template in synthesizing MgO is beneficial toward adsorbent physicochemical properties and further expected leading to the improvement of adsorbent's CO<sub>2</sub> capture performance.

In this study, the lime (*Citrus aurantifolia*) peel template was utilized as a template in the preparation of mesoporous MgO adsorbent (MgO-LPT). The prepared adsorbents were characterized using N<sub>2</sub> physisorption, Fourier transform infrared spectroscopy (FTIR), and thermogravimetric analysis (TGA). The CO<sub>2</sub> uptake capacities of the adsorbents were investigated under pure CO<sub>2</sub> and ambient pressure and temperature conditions.

## 2. Materials and Methods

### 2.1 Materials

All chemical reagents, such as magnesium nitrate hexahydrate (Mg(NO<sub>3</sub>)<sub>2</sub>·6H<sub>2</sub>O) (99.5%), ethylene glycol (C<sub>2</sub>H<sub>6</sub>O<sub>2</sub>) (99.5%), and ammonia solution 28% (NH<sub>3</sub>), used in this study were purchased from QREC (Asia) SDN BHD. Lime peel was obtained from the local market.

### 2.2 Preparation of MgO-LPT

LPT was acquired from lime waste and washed three times to remove impurities. The LPT was then dried overnight at 110 °C and roughly crushed to reduce the template size to approximately less than 0.5 mm × 0.5 mm. Templating was initiated by weighing 20 g of Mg(NO<sub>3</sub>)<sub>2</sub>·6H<sub>2</sub>O and then adding it to 200 mL C<sub>2</sub>H<sub>6</sub>O<sub>2</sub>. Subsequently, the mixture was stirred for 10 min and sonicated for 10 min to ensure the complete dissolution of Mg(NO<sub>3</sub>)<sub>2</sub>·6H<sub>2</sub>O. Thereafter, 3 g dried LPT was immersed in the abovementioned solution and stirred for 1 h.

The pH of the mixture was set to 10 using  $\text{NH}_3$ , and the resulting mixture was stirred for another 30 min. The MgO-absorbed LPT was then filtered and dried for 1 h at 110 °C. Next, the dried MgO-absorbed LPT was calcined at 600 °C for 4 h and ground to achieve powdered MgO-LPT.

### 2.3 Preparation of MgO-TD

$\text{Mg}(\text{NO}_3)_2 \cdot 6\text{H}_2\text{O}$  (20 g) was directly calcined at 600 °C for 3 h, and then, the calcined residue was ground to obtain powdered MgO-TD.

### 2.4 Characterization

Surface functional groups of the prepared adsorbents were determined by FTIR using a Cary 600 series spectrometer in the mid-infrared range of 400–4000  $\text{cm}^{-1}$ . The thermal decomposition behavior of the prepared adsorbents was evaluated via TGA in the temperature range of 30–900 °C at a scan rate of 10 °C  $\text{min}^{-1}$  using PerkinElmer STA 8000.  $\text{N}_2$  adsorption-desorption isotherms were acquired using a gas sorption analyzer (Quantachrome Instruments, Autosorb IQ, version 3.0) to investigate the textural properties of the adsorbents, and the data were analyzed using the 3Flex 5.0 software.

### 2.5 Measurement of $\text{CO}_2$ Adsorption

$\text{CO}_2$  adsorption was measured using a fixed-bed U-shaped adsorption column equipped with a  $\text{CO}_2$  analyzer (Quantek Instruments Model 906). The schematic diagram of the  $\text{CO}_2$  adsorption testing setup was shown in Figure 1. Before adsorption, the adsorbent (50 mg) was pre-treated at 150 °C for 1 h under nitrogen flow (20  $\text{mL} \cdot \text{min}^{-1}$ ) to remove any pre-adsorbed atmospheric gases. Next, the adsorption testing was conducted on pre-treated adsorbent under

pure  $\text{CO}_2$  condition at ambient pressure and temperature for 1 h. Subsequently, the adsorbent was desorbed under nitrogen flow (20  $\text{mL} \cdot \text{min}^{-1}$ ) at 150 °C for 30 min.  $\text{CO}_2$  desorbed from the adsorbent was quantified using the area under the adsorption-desorption curve. The  $\text{CO}_2$  uptake capacity of the adsorbents was calculated using the mean of the results of three adsorption-desorption cycles.

## 3. Results and Discussions

### 3.1 Characterization

FTIR spectra of the prepared adsorbents were recorded in the wavelength range of 400–4000  $\text{cm}^{-1}$ . As shown in Figure 2, the spectrum of MgO-LPT exhibits several intense absorption peaks as compared to that of MgO-TD. The sharp absorption peak at 3690  $\text{cm}^{-1}$  and broad vibration band at 3440–3450  $\text{cm}^{-1}$  are attributed to the stretching vibration of the hydroxyl ( $-\text{OH}$ ) group on the crystal face of the low-coordination site or defect site and residual water, respectively [12,13]. This indicates that MgO-LPT possesses more OH groups than those of MgO-TD, which can lead to the formation of a large amount of bicarbonate on MgO-LPT. The spectra of both adsorbents show a peak at 2370  $\text{cm}^{-1}$ , which is associated with the existence of a  $\text{CO}_2$  molecule [14]. Compared to the case of MgO-TD, the intensity of the 2370  $\text{cm}^{-1}$  peak of MgO-LPT decreased because of the use of high-intensity incident light due to the high bond population of MgO-LPT [15]. Moreover, the spectrum of MgO-LPT demonstrates more prominent peaks associated with the adsorbed atmospheric  $\text{CO}_2$  than that of MgO-TD. These peaks are located at 870  $\text{cm}^{-1}$ , 1050  $\text{cm}^{-1}$  and 1430–1450  $\text{cm}^{-1}$ , and 1655  $\text{cm}^{-1}$ , which are assigned to the existence of monodentate carbonate, bicarbonate, and bidentate

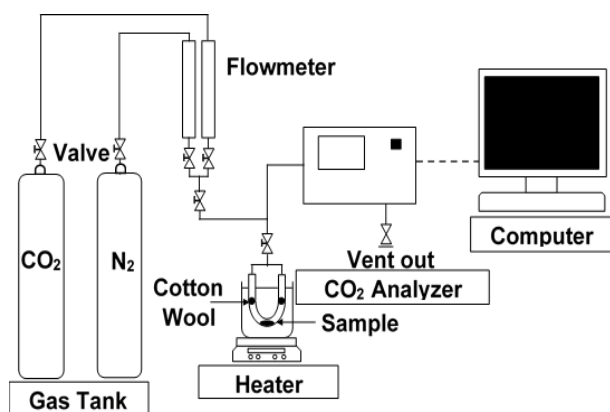


Figure 1. Schematic diagram of  $\text{CO}_2$  adsorption testing setup.

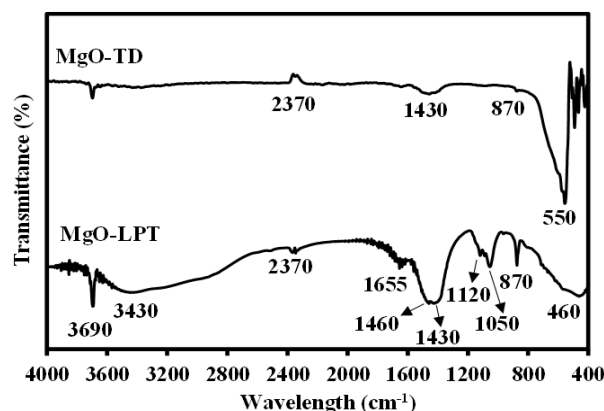


Figure 2. FTIR spectra of MgO-TD and MgO-LPT.

carbonate, respectively [12,16–18]. Furthermore, the band at  $1120\text{ cm}^{-1}$  was attributed to the  $\nu_1$  symmetric stretching vibration of  $\text{CO}_3^{2-}$  [19]. The more intense peaks corresponding to carbonate species in the spectrum of MgO-LPT suggest that MgO-LPT possesses more active sites, leading to high  $\text{CO}_2$  uptake capacity. The sharp peak at  $550\text{ cm}^{-1}$  observed for MgO-TD and the strong peak at  $460\text{ cm}^{-1}$  obtained for MgO-LPT corresponds to the stretching vibration of Mg-O [20,21].

As shown in Figure 3(a and b), MgO-TD and MgO-LPT demonstrate different decomposition behaviors. This might be owing to the different chemical compositions of the chemical reagents and templates used during the preparation of these adsorbents. Both adsorbents exhibited initial weight loss at  $<200\text{ }^\circ\text{C}$ , corresponding to the removal of residual moisture; this indicated

that MgO-LPT had a higher residual moisture content than that of MgO-TD. During the second degradation stage ( $250\text{--}600\text{ }^\circ\text{C}$ ), MgO-TD showed a higher weight loss of 27 wt% as compared to that of MgO-LPT (only approximately 9 wt%) (Table 1). This might imply that MgO-TD possesses more organic residues than those of MgO-LPT. During the third stage of degradation, MgO-LPT exhibited more weight loss than that of MgO-TD, probably because of the removal of carbon residue, also known as fixed carbon, from the template. As MgO-LPT was prepared at  $600\text{ }^\circ\text{C}$ , a small amount of fixed carbon was still present in it as fixed carbon remains stable at high temperatures ( $700\text{ }^\circ\text{C}$ ) [11].

$\text{N}_2$  adsorption-desorption measurements were carried out to investigate the structural properties of the adsorbents. Figure 4(a and b)

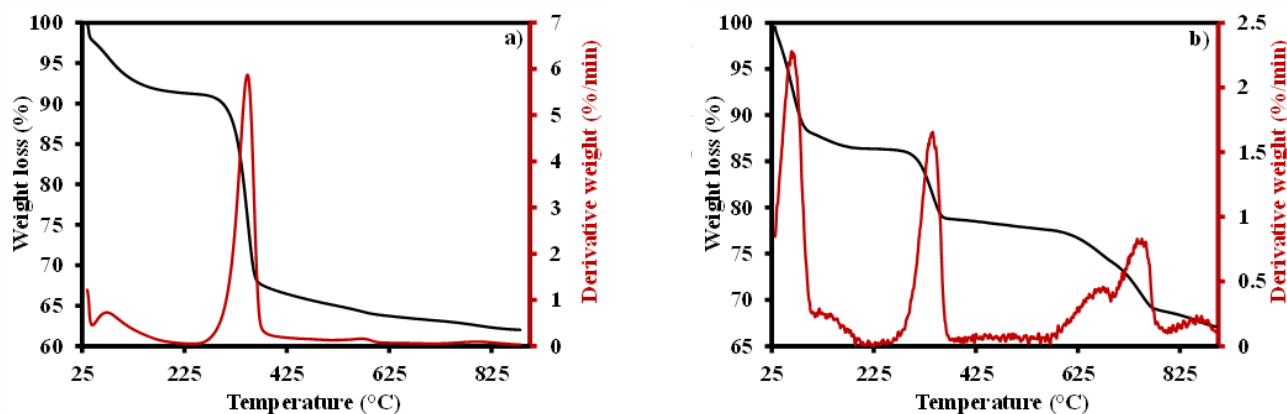


Figure 3. TGA/DTG curve of a) MgO-TD and b) MgO-LPT.

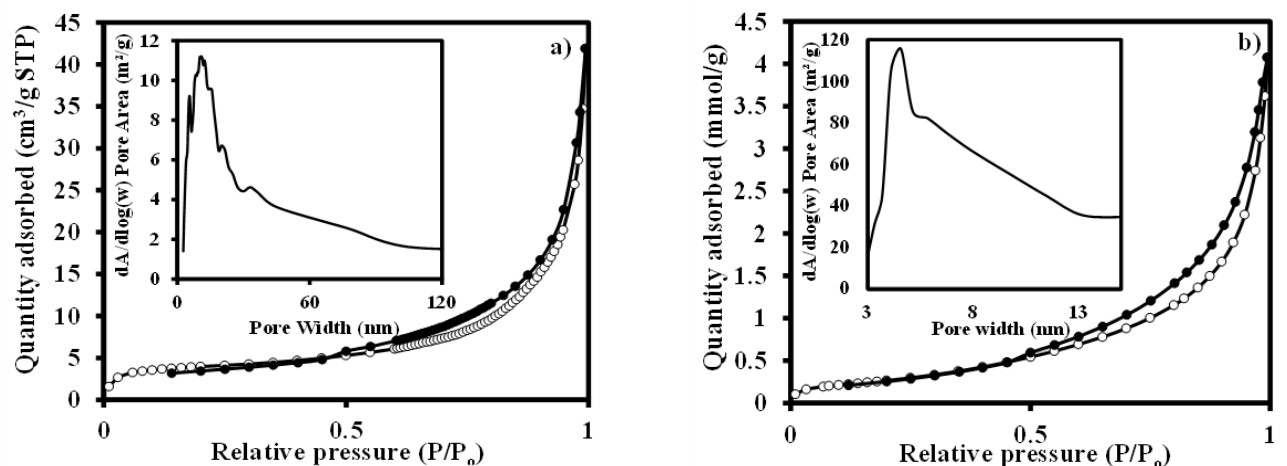
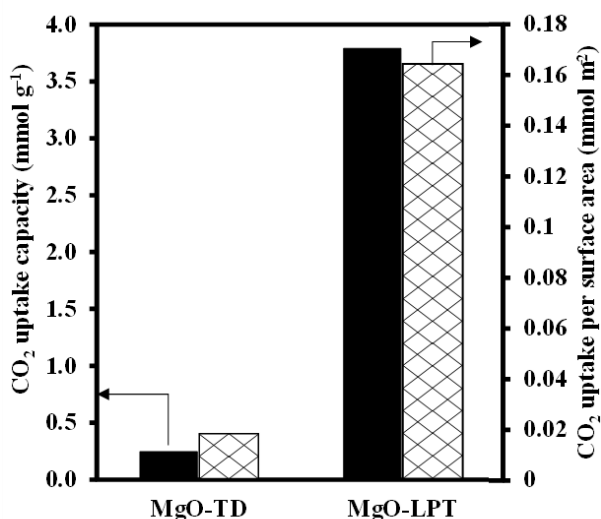


Figure 4.  $\text{N}_2$  adsorption-desorption isotherm of a) MgO-TD and b) MgO-LPT.

Table 1. Summary of the thermal decomposition behaviors of MgO-TD and MgO-LPT.

Adsorbent	Weight loss (wt%)			Total weight loss (wt%)
	$<200\text{ }^\circ\text{C}$	$\sim 600\text{ }^\circ\text{C}$	$>600\text{ }^\circ\text{C}$	
MgO-TD	9	27	2	38
MgO-LPT	14	9	11	34

show that both adsorbents exhibit type IV isotherms with H3 hysteresis loops. This implies that the adsorbents mainly contain mesopores, and the pores are mostly disordered slit pores resulting from the stacking of sheets or particles [22]. The hysteresis loops of the isotherms of both adsorbents were observed in the P/P<sub>0</sub> range of 0.45–1.0. Due to the LPT, the specific surface area of MgO-LPT increased (23 m<sup>2</sup>.g<sup>-1</sup>) as compared to that of MgO-TD (only 13 m<sup>2</sup>.g<sup>-1</sup>). Moreover, the Barrett – Joyner – Halenda pore volume and pore diameter of



**Figure 5.** CO<sub>2</sub> uptake capacity of MgO-TD and MgO-LPT.

MgO-LPT increased as compared to those of MgO-TD (Table 2). Thus, the LPT biotemplating improved the structural properties of MgO-LPT and thereby led to the high CO<sub>2</sub> uptake capacity of MgO-LPT. This surface area enhancement resulted from the utilization of citrus fruit peel as a template also observed in several studies reported [23,24]. For instances, Zhao *et al.* has reported in the synthesizing of the hierarchically porous LaFeO<sub>3</sub> sample from the pomelo peel as a template [23]. It is found that the LaFeO<sub>3</sub> sample exhibited enhanced textural properties than the LaFeO<sub>3</sub> sample prepared without pomelo peel as a template. Thus, this enhanced textural property has resulted in better catalytic performance than another prepared sample. This revealed that the utilization of bio-material such as citrus fruit species as a template could improve the adsorbent's structural properties, which consequently influence its performance.

### 3.2 CO<sub>2</sub> Uptake Capacity

CO<sub>2</sub> uptake capacity was examined under CO<sub>2</sub> gas and ambient conditions to evaluate the relationship between the structural properties and uptake performance. As shown in Figure 5, MgO-LPT demonstrated a CO<sub>2</sub> uptake capacity of 3.79 mmol CO<sub>2</sub>.g<sup>-1</sup>, which was 15 times that of MgO-TD. This was attributed to the enhanced surface area of MgO-LPT. The

**Table 2.** Textural properties of MgO-TD and MgO-LPT.

Adsorbent	Surface area (m <sup>2</sup> .g <sup>-1</sup> )	Pore volume (cm <sup>3</sup> .g <sup>-1</sup> )	Pore diameter (nm)
MgO-TD	13	0.065	19
MgO-LPT	23	0.142	25

**Table 3.** Textural properties and CO<sub>2</sub> uptake capacities of the MgO adsorbents fabricated by various methods.

Adsorbent	Synthesis method	Surface area (m <sup>2</sup> .g <sup>-1</sup> )	Pore volume (cm <sup>3</sup> .g <sup>-1</sup> )	Adsorption temperature (°C)	CO <sub>2</sub> uptake (mmol.g <sup>-1</sup> )	Ref.
MgO-TD	Thermal decomposition method	13	0.065	298	0.247	This work
MgO-LPT	Lime peel biotemplating	23	0.142	298	3.79	This work
MgO	Double-replicate	250	0.53	298	1.82	[28]
MgO	Precipitation method	331	0.575	298	1.56	[29]
MgO	Aerogel method	686	2.11	303	2.34	[30]
MgO-A	Sol-gel method	350	0.414	303	0.681	[31]
MgO-O	Sol-gel method	149	0.598	303	0.568	[31]
MgO-N	Sol-gel method	124	0.546	303	0.545	[31]

increased surface area of an adsorbent can cause the exposure of more active sites, thus promoting the attachment of more CO<sub>2</sub> [1,25]. This correlation between enhanced adsorbent's surface area and CO<sub>2</sub> uptake capacity also observed in several studies reported. For instances, Guo *et al.* has successfully fabricated MgO adsorbents through different preparation method [22]. It is found that each preparation method has resulted in different morphological features. The MgO adsorbent prepared via solid-state chemical reaction (MgO-SR) has exhibited a sheet-like with higher surface area compared to other prepared samples, which consequently increase the adsorbent's surface-active site. This MgO-SR's structural properties enhancement has contributed to the higher CO<sub>2</sub> uptake capacity than those of prepared MgO adsorbent.

In addition, although MgO-LPT has the smallest surface area than those of the other MgO adsorbents reported in the literature (Table 3), it still exhibits the highest CO<sub>2</sub> uptake capacity per surface area (0.165 mmol.m<sup>-2</sup>) as compared to those of the other MgO adsorbents. This may be because of the presence of rich surface defects on MgO-LPT. This LPT bio-templating might contribute to the generation of point defects such as cationic vacancies and low-coordination anionic sites. The corner, step, and edge sites are the low-coordination anionic sites of MgO, which are highly polarizable [26] and exhibit high Lewis basicity. The Lewis basicity is the ability of the adsorbent surface to donate an electron pair to the CO<sub>2</sub> (Lewis acid) molecule and form a carbonate species [27]. This supported the FTIR results, that is, the spectrum of MgO-LPT exhibited more bands corresponding to the carbonate species than those of MgO-TD. It can be concluded that MgO-LPT possesses higher surface reactivity, which results in the easy adsorption of atmospheric CO<sub>2</sub>, than that of MgO-TD.

#### 4. Conclusions

In this study, mesoporous MgO-LPT was successfully fabricated using the LPT as a template. The utilization of LPT has demonstrated the enhancement of adsorbent's structural properties, which MgO-LPT exhibited a higher specific surface area and pore volume as compared to MgO-TD. The improved MgO-LPT surface area has contributed to the high CO<sub>2</sub> uptake capacity of 3.79 mmol CO<sub>2</sub>.g<sup>-1</sup>, which is 15-times that of MgO-TD. In addition, even though the surface area of MgO-LPT is the

smallest as compared to those of several previously reported MgO adsorbents, the CO<sub>2</sub> uptake capacity of MgO-LPT was the highest than those of the other MgO adsorbents. Therefore, this study reveals that lime (*Citrus aurantifolia*) peel is a promising, inexpensive template source for the synthesis of mesoporous MgO with high CO<sub>2</sub> uptake capacity.

#### Acknowledgements

This work was supported by the Universiti Teknologi Malaysia (Grant No. 16J64) and Ministry of Higher Education Malaysia through the Fundamental Research Grant Scheme (FRGS) Grant No. FRGS/1/2019/STG07/UTM/02/8 (Grant No. 5F217).

#### References

- [1] Ruhaimi, A.H., Aziz, M.A.A., Jalil, A.A. (2021). Magnesium oxide-based adsorbents for carbon dioxide capture: Current progress and future opportunities. *Journal of CO<sub>2</sub> Utilization*, 43, 101357. DOI: 10.1016/j.jcou.2020.101357
- [2] Modak, A., Jana, S. (2019). Advancement in porous adsorbents for post-combustion CO<sub>2</sub> capture. *Microporous and Mesoporous Materials*, 276, 107–132. DOI: 10.1016/j.micromeso.2018.09.018
- [3] Songolzadeh, M., Ravanchi, M.T., Soleimani, M. (2012). Carbon Dioxide Capture and Storage: A General Review on Adsorbents. *International Journal of Chemical and Molecular Engineering*, 6(10), 900–907. DOI: 10.5281/zenodo.1076266
- [4] Azmi, A.A., Ruhaimi, A.H., Aziz, M.A.A. (2020). Efficient 3-aminopropyltrimethoxysilane functionalised mesoporous ceria nanoparticles for CO<sub>2</sub> capture. *Materials Today Chemistry*, 16, 100273. DOI: 10.1016/j.mtchem.2020.100273
- [5] Hu, Y., Guo, Y., Sun, J., Li, H., Liu, W. (2019). Progress in MgO sorbents for cyclic CO<sub>2</sub> capture: a comprehensive review. *Journal of Materials Chemistry A*, 7(35), 20103–20120. DOI: 10.1039/C9TA06930E
- [6] Gao, W., Zhou, T., Gao, Y., Louis, B., O'Hare, D., Wang, Q. (2017). Molten salts-modified MgO-based adsorbents for intermediate-temperature CO<sub>2</sub> capture: A review. *Journal of Energy Chemistry*, 26(5), 830–838. DOI: 10.1016/j.jechem.2017.06.005
- [7] Azmi, A.A., Ngadi, N., Kamaruddin, M.J., Zakaria Z.Y., Teh, L.P., Rozali Annuar, N.H., Setiabudi, H.D., Ab Aziz, M.A. (2019). Rapid one pot synthesis of mesoporous ceria nano-

- particles by sol-gel method for enhanced CO<sub>2</sub> capture. *Chemical Engineering Transactions*, 72, 403–408. DOI: 10.3303/CET1972068
- [8] Wang, J., Li, M., Lu, P., Ning, P., Wang, Q. (2019). Kinetic study of CO<sub>2</sub> capture on ternary nitrates modified MgO with different precursor and morphology. *Chemical Engineering Journal*, 392, 123752. DOI: 10.1016/j.cej.2019.123752
- [9] Abarna, B., Preethi, T., Karunanithi, A., Rajarajeswari, G. (2016). Influence of jute template on the surface, optical and photocatalytic properties of sol-gel derived mesoporous zinc oxide. *Materials Science in Semiconductor Processing*, 56, 243–250. DOI: 10.1016/j.mssp.2016.09.004
- [10] Chen, G., Yang, X., Miao, K., Long, M., Deng, W. (2017). Root hairs as biotemplates for fabricating hollow double-layer CuO microtubes. *Materials Letters*, 194, 193–196. DOI: 10.1016/j.matlet.2017.02.035
- [11] Pathak, P.D., Mandavgane, S.A., Kulkarni, B.D. (2017). Fruit peel waste: characterization and its potential uses. *Current Science*, 113(3), 444–454. DOI: 10.18520/CS/V113/I03/444-454.
- [12] Selvam, N.C.S., Kumar, R.T., Kennedy, L.J., Vijaya, J.J. (2011). Comparative study of microwave and conventional methods for the preparation and optical properties of novel MgO-micro and nano-structures. *Journal of Alloys and Compounds*, 509(41), 9809–9815. DOI: 10.1016/j.jallcom.2011.08.032
- [13] Jeon, H., Min, Y.J., Ahn, S.H., Hong, S.M., Shin, J.S., Kim, J.H., Lee, K.B. (2012). Graft copolymer templated synthesis of mesoporous MgO/TiO<sub>2</sub> mixed oxide nanoparticles and their CO<sub>2</sub> adsorption capacities. *Colloids and Surfaces A: Physicochemical and Engineering Aspects*, 414, 75–81. DOI: 10.1016/j.colsurfa.2012.08.009
- [14] Bazhan, Z., Ghodsi, F.E., Mazloom, J. (2013). Effect of stabilizer on optical and structural properties of MgO thin films prepared by sol-gel method. *Bulletin of Materials Science*, 36(5), 899–905. DOI: 10.1007/s12034-013-0554-0
- [15] Fuqua, P.D., Mansour, K., Alvarez Jr, D., Marder, S.R., Perry, J.W., Dunn, B.S. (1992). Synthesis and nonlinear optical properties of sol-gel materials containing phthalocyanines. In *SPIE Proceedings: Sol-Gel Optics II*, 1758. San Diego, CA, United States. DOI: 10.1117/12.132042
- [16] Yang, N., Ning, P., Li, K., Wang, J. (2018). MgO-based adsorbent achieved from magnesite for CO<sub>2</sub> capture in simulate wet flue gas. *Journal of the Taiwan Institute of Chemical Engineers*, 86, 73–80. DOI: 10.1016/j.jtice.2018.02.006
- [17] Ding, Y.D., Song, G., Liao, Q., Zhu, X., Chen, R. (2016). Bench scale study of CO<sub>2</sub> adsorption performance of MgO in the presence of water vapor. *Energy*, 112, 101–110. DOI: 10.1016/j.energy.2016.06.064
- [18] Kwon, H.K., Park, D.G. (2009). Infra-red study of surface carbonation on polycrystalline magnesium hydroxide. *Bulletin of the Korean Chemical Society*, 30(11), 2567–2573. DOI: 10.5012/bkcs.2009.30.11.2567
- [19] Botha, A., Strydom, C. (2003). DTA and FT-IR analysis of the rehydration of basic magnesium carbonate. *Journal of Thermal Analysis and Calorimetry*, 71(3), 987–996. DOI: 10.1023/A:1023355016208
- [20] Li, P., Lin, Y., Chen, R., Li, W. (2020). Construction of a hierarchical-structured MgO-carbon nanocomposite from a metal-organic complex for efficient CO<sub>2</sub> capture and organic pollutant removal. *Dalton Transactions*. DOI: 10.1039/D0TD00722F
- [21] Sutapa, I.W., Wahab, A.W., Taba, P., La Nafie, N. (2018). Synthesis and structural profile analysis of the MgO nanoparticles produced through the sol-gel method followed by annealing process. *Oriental Journal of Chemistry*, 34(2), 1016. DOI: 10.13005/ojc/340252
- [22] Guo, Y., Tan, C., Wang, P., Sun, J., Li, W., Zhao, C., Lu, P. (2020). Structure-performance relationships of magnesium-based CO<sub>2</sub> adsorbents prepared with different methods. *Chemical Engineering Journal*, 379, 122277. DOI: 10.1016/j.cej.2019.122277
- [23] Zhao, S., Wang, L., Wang, Y., Li, X. (2018). Hierarchically porous LaFeO<sub>3</sub> perovskite prepared from the pomelo peel bio-template for catalytic oxidation of NO. *Journal of Physics and Chemistry of Solids*, 116, 43–49. DOI: 10.1016/j.jpcs.2017.12.057
- [24] Zhao, R., Zhang, X., Peng, S., Hong, P., Zou, T., Wang, Z., Xing, X., Wang, Y. (2020). Shaddock peels as bio-templates synthesis of Cd-doped SnO<sub>2</sub> nanofibers: A high performance formaldehyde sensing material. *Journal of Alloys and Compounds*, 813, 152170. DOI: 10.1016/j.jallcom.2019.152170
- [25] Tian, P., Han, X.Y., Ning, G.L., Fang, H.X., Ye, J.W., Gong, W.T., Lin, Y. (2013). Synthesis of porous hierarchical MgO and its superb adsorption properties. *ACS Applied Materials and Interfaces*, 5(23), 12411–12418. DOI: 10.1021/am403352y
- [26] Montero, J., Isaacs, M., Lee, A., Lynam, J., Wilson, K. (2016). The surface chemistry of nanocrystalline MgO catalysts for FAME production: An in situ XPS study of H<sub>2</sub>O, CH<sub>3</sub>OH and CH<sub>3</sub>OAc adsorption. *Surface Science*, 646, 170–178. DOI: 10.1016/j.susc.2015.07.011

- [27] Cornu, D., Guesmi, H., Krafft, J.M., Lauron-Pernot, H. (2012). Lewis Acido-Basic Interactions between CO<sub>2</sub> and MgO Surface: DFT and DRIFT Approaches. *The Journal of Physical Chemistry C*, 116(11), 6645–6654. DOI: 10.1021/jp211171t
- [28] Bhagiyalakshmi, M., Lee, J.Y., Jang, H.T. (2010). Synthesis of mesoporous magnesium oxide: its application to CO<sub>2</sub> chemisorption. *International Journal of Greenhouse Gas Control*, 4(1), 51–56. DOI: 10.1016/j.ijggc.2009.08.001
- [29] Tuan, V.A., Lee, C.H. (2018). Preparation of rod-like MgO by simple precipitation method for CO<sub>2</sub> capture at ambient temperature. *Vietnam Journal of Chemistry*, 56(2), 197–202. DOI: 10.1002/vjch.201800013
- [30] Ho, K., Jin, S., Zhong, M., Vu, A.T., Lee, C.H. (2017). Sorption capacity and stability of mesoporous magnesium oxide in post-combustion CO<sub>2</sub> capture. *Materials Chemistry and Physics*, 198, 154–161. DOI: 10.1016/j.matchemphys.2017.06.002
- [31] Alkadhém, A.M., Elgzoly, M.A.A., Onaizi, S.A. (2020). Novel Amine-Functionalized Magnesium Oxide Adsorbents for CO<sub>2</sub> Capture at Ambient Conditions. *Journal of Environmental Chemical Engineering*, 8(4), 103968. DOI: 10.1016/j.jece.2020.103968

*Selected and Revised Papers from International Conference on Sustainable Energy and Catalysis 2021 (ICSEC 2021) (<https://engineering.utm.my/chemicalenergy/icsec2021/>) (School of Chemical and Energy Engineering, Faculty of Engineering, Universiti Teknologi Malaysia, 16-17<sup>th</sup> February 2021) after Peer-reviewed by Scientific Committee of ICSEC 2021 and Peer-Reviewers of Bulletin of Chemical Reaction Engineering & Catalysis. Editors (Guest) in this ICSEC 2021 section are Nor Aishah Saidina Amin, Mohd Asmadi Mohammed Yussuf, Salman Raza Naqvi, while Editor in Chief is I. Istadi.*